

# Aggregation of Published Non-Uniform Axial Power Data for Phase II of the OECD/NEA AI/ML Critical Heat Flux Benchmark

Reece Bourisaw<sup>1</sup>, Reid McCants<sup>1</sup>, Jean-Marie Le Corre<sup>2</sup>, Anna Iskhakova<sup>1</sup> and Arsen S. Iskhakov<sup>1</sup>

<sup>1</sup>Department of Mechanical and Nuclear Engineering, Kansas State University, Manhattan, KS,

<sup>2</sup>Westinghouse Electric Sweden AB, 72163 Västerås, Sweden

[rbourisaw@ksu.edu](mailto:rbourisaw@ksu.edu)

[Placeholder for Digital Object Identifier (DOI) to be added by ANS]

## INTRODUCTION

Critical heat flux (CHF) is a key thermal-hydraulic phenomenon in which the two-phase coolant’s heat-transfer capability drops abruptly, establishing the thermal-design limit, defined as the departure from nucleate boiling (DNB) in pressurized water reactors (PWRs) and as the critical-power condition in boiling water reactors (BWRs) [1]. Therefore, accurate prediction of CHF is essential for setting safe operating margins and maximizing reactor power output without risking fuel damage. However, CHF modeling remains challenging due to the complex coupling of local two-phase hydrodynamics, surface characteristics, transient thermal boundary-layer development, and geometric influences, factors that vary widely with pressure, flow rate, and heating profile [2, 3].

Traditional CHF correlations often rely on simplified mechanistic assumptions, empirical parametric relationships or look-up tables (LUT), which can limit their accuracy and adaptability under novel or strongly non-uniform heating conditions [4, 5]. Machine learning (ML) methods, by contrast, can learn high-dimensional patterns directly from large datasets and have demonstrated improved accuracy and robustness in CHF prediction [6]. However, many ML-based CHF studies have been carried out independently as proof-of-concept demonstrations on limited or proprietary datasets, underscoring the need for coordinated benchmarking efforts. To address this, the Organization for Economic Co-operation and Development / Nuclear Energy Agency (OECD/NEA) Task Force on Artificial Intelligence and Machine Learning for Scientific Computing in Nuclear Engineering organized a CHF benchmark to provide common datasets, blind-test partitions, and reproducible evaluation protocols for evaluating ML-based CHF predictors [7].

Phase I of the CHF benchmark, as specified in [7], comprised four tasks: (1) dimensionality analysis for feature selection and extraction; (2) development and optimization of ML-based CHF regression models based on the Nuclear Regulatory Commission (NRC) database; (3) rigorous model evaluation and uncertainty quantification (UQ); and (4) independent blind testing on withheld data. While Phase I demonstrated the feasibility of AI/ML approaches for CHF prediction under uniform heating, it remained limited by the absence of spatially varying power profiles. Phase II will extend the CHF benchmark to include more complex geometries and boundary conditions, to be used along with transfer learning techniques, advanced UQ, and design optimization, all of which require a

richer, more diverse CHF dataset.

To support these Phase II tasks, Kansas State University, in collaboration with Westinghouse Electric Sweden, collected additional CHF measurements in tubes with uniform and non-uniform axial power distributions within the ME 535 “Interdisciplinary Industrial Design Project II” course. This paper reports on those activities and describes the newly digitized uniform and non-uniform CHF datasets; more details can be found in the report [8].

## DATA COLLECTION AND ORGANIZATION

### Data Source and Characteristics

The primary source of the experimental data collected comes from the Korea Atomic Energy Research Institute (KAERI) technical report [9]. The report investigates how axial heat flux distribution affects the occurrence of CHF in boiling systems. The study includes an extensive set of experimental CHF measurements under both uniform and non-uniform heating conditions, providing valuable data for understanding and modeling CHF behavior in nuclear thermal-hydraulic systems.

Overall, 1539 CHF test cases were collected/digitized from [9], comprising 651 uniform heating measurements and 888 non-uniform heating cases, summarized in Table I. The experimental setups used water coolant in vertical round tubes with internal diameter of 5.44 – 28.3 mm and heated lengths of 0.061 – 7.0 m.

TABLE I: Summary of the collected data.

Heating	Pressure, MPa	Mass flux, kg/(m <sup>2</sup> ·s)	Equilibrium quality at CHF
Uniform	0.43 – 18	335.0 – 9561.9	–0.582 – 0.901
Non-uniform	0.43 – 18	328.2 – 8916.0	–0.952 – 0.924

The non-uniform subset encompasses a variety of axial heat flux profiles. Representative examples of digitized profiles, adapted from one of the original sources [10], are shown in Fig.1. These profiles can generally be classified as “spike”, “middle-peaked”, or shifted toward the “inlet” or “outlet”.

### Data Collection Workflow

The uniform heating data were directly extracted from the KAERI report. For the non-uniform heating, we digitized heating profiles from the KAERI figures using WebPlotDigi-

tizer [11] with the following steps:

1. *Outliers removal*: Spurious clicks in the published curves were manually discarded.
2. *Interpolation*: Piecewise cubic Hermite interpolation (PCHIP) mapped each profile onto a uniform 40-node axial mesh.
3. *Energy balance check*: The integrated axial flux was compared to published total power; cases with  $>2\%$  discrepancy were reprocessed.

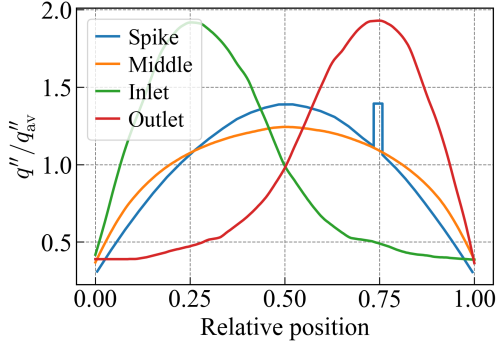


Fig. 1: Examples of the collected heat flux profiles.  $q''$  denotes the heat flux,  $q''_{av}$  denotes the average heat flux.

For the uniform cases, inlet subcooling and outlet quality are reported in the KAERI report [9]. The remaining inlet and outlet parameters were calculated using IAPWS thermodynamic properties [12]. Unlike the non-uniform cases, the uniform data did not use a detailed 40-node mesh; instead, only inlet and outlet values of local power and temperature/equilibrium quality are recorded. In the non-uniform dataset, the inlet temperature is provided and, combined with the specified heat flux distribution, was used to compute all thermodynamic parameters along the heated tube on a uniform 40-node mesh.

## Dataset Structure

The quantities were saved in separate (uniform and non-uniform) XML files which are easily readable by computer scripts, see Table II that describes the saved quantities. The open-source XML files can be accessed in [13]. Such database can be used to develop and validate predictive CHF models, in particular with respect to the effect of axial power distribution.

## PRELIMINARY MODELING EFFORTS

### Traditional Correlations

We first tested traditional CHF correlations, such as those by Bowring [14]:

$$q''_{cr} = \frac{A - B h_{fg} x}{C},$$

and Biasi [15]:

$$q''_{cr} = 15.048 \times 10^7 (100 D)^{-n} G^{-0.6} H (1 - x),$$

where  $A$ ,  $B$ ,  $C$  and  $H$  are empirical parameters that depend on the thermodynamic state, flow conditions and geometric

factors,  $h_{fg}$  is the latent heat of vaporization,  $x$  is the steam quality,  $D$  is the hydraulic diameter,  $G$  is the mass flow rate.

These correlations were used to predict the collected dataset and were evaluated separately for uniform and non-uniform heating conditions. For uniform cases, Bowring's correlation yields a root mean square error (RMSE) of 27%, which increases significantly to 74% for non-uniform cases. Biasi's correlation performs worse, with an RMSE of 62% for uniform cases and 74% for non-uniform ones. Both models occasionally produce unphysical (negative) CHF values, particularly near the limits of their applicability, and exhibit a systematic bias in predicting the CHF location under non-uniform heating. In contrast, the LUT [5], including a non-uniform axial heat flux correction factor [1], demonstrates better overall performance, achieving a lower RMSE of approximately 20% for uniform cases and maintaining greater robustness under non-uniform conditions, with an RMSE of 36%, see Fig. 2.

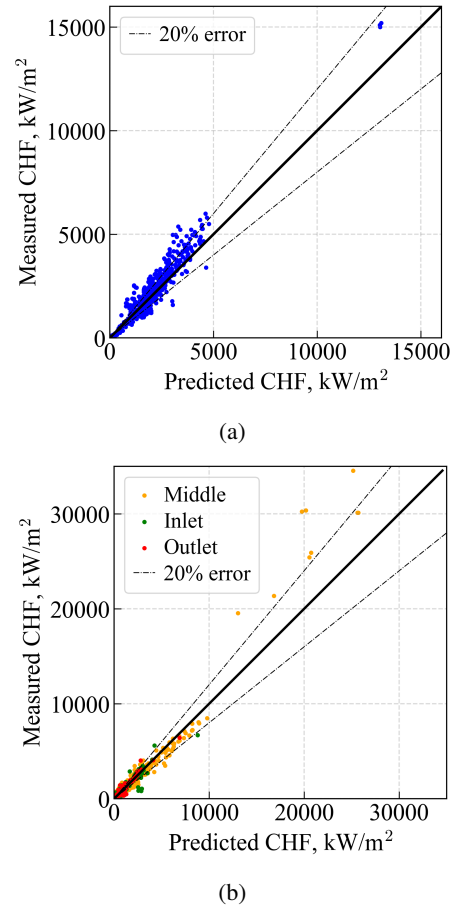


Fig. 2: Predicted vs. measured CHF using LUT for (a) uniform data, (b) non-uniform data.

### Neural Network Modeling

A feedforward neural network (NN) was implemented following architecture by [6], see Table III. The inputs comprised tube diameter, heated length, pressure, mass flux and equilibrium quality. The NN was trained to predict the CHF

TABLE II: Quantities saved for each test case.

Parameter	Keyword	Units / Note
Test #	<TestID>	Sequential (e.g., from 1 to 651 for uniform)
Internal tube diameter	<Diameter>	[m]
Wetted perimeter	<Perimeter>	[m]
Flow area	<Area>	[m <sup>2</sup> ]
Total heated length	<Length>	[m]
Pressure	<Pressure>	[Pa]
Total power	<Power>	[W]
Mass flux	<MassFlux>	[kg/(m <sup>2</sup> ·s)]
Mass flow rate	<MassFlow>	[kg/s]
Inlet temperature	<InletTemperature>	[°C]
Inlet enthalpy	<InletEnthalpy>	[J/kg]
Average heat flux, $q''_{av}$	<HeatFlux>	[W/m <sup>2</sup> ]
Coolant	<Fluid>	Water only
Original data source	<Source>	Original reference within [9] (e.g., “Swenson”)
Normalized local power $q''(z)/q''_{av}$	<WallPower>	[-], 40 non-uniform values or 2 uniform values
Mesh space, $\Delta z$	<WallMesh>	[m], 40 non-uniform values or 2 uniform values
Equilibrium quality, $x(z)$	<EquilibriumQuality>	[-], 40 non-uniform values or 1 uniform value (outlet)
Mesh coordinate, $z$	<QualityPosition>	[m], 40 non-uniform values or 1 uniform value (outlet)
<b>Additional Non-Uniform Entries</b>		
CHF coordinate	<CHFLocation>	[m]
Power shape	<Shape>	e.g., “spike”
Continuity of the profile	<Continuous>	“yes” or “no” (for integration or interpolation purposes)

value on the uniform subset and achieved relatively high accuracy in predicting the held out uniform data. When this NN was used to predict the non-uniform CHF data, the accuracy significantly degraded, see Fig. 3. This confirms that further enhancements are needed to fully capture spatial CHF behavior under strong axial non-uniformity, which will be addressed in the future work within the Phase II of the CHF benchmark.

TABLE III: Hyperparameters and NN architecture.

Parameter	Value / Method
Number of layers and neurons	5 – 61 – 51 – 28 – 39 – 26 – 21 – 20 – 14 – 1
Activation	ReLU
Optimizer	Adam
Loss function	Mean squared error
Regularization	Dropout 1% after the first layer
Learning rate	0.01 with decay on plateau

## CONCLUSIONS

In this study, we assembled and digitized a comprehensive CHF dataset of 1539 cases, including 651 uniform and 888 non-uniform profiles, sourced from KAERI technical report. Uniform and non-uniform subsets were encoded in separate XML files compliant with the CHF benchmark. For each experimental measurement all necessary parameters were recorded, including geometry, thermodynamic conditions, axial flux distributions, and additional metadata. Preliminary modeling

confirmed that the LUT outperforms classical correlations on both uniform and non-uniform data. A feedforward NN was trained on uniform data and used to predict both subsets. These results confirmed the accuracy of the ML models to predict the uniform data, while for the non-uniform data additional consideration are required to take into account the axial heat flux distributions. Future work activities will be aligned with the CHF benchmark Phase II priorities.

## ACKNOWLEDGMENTS

This work was conducted within ME 575 “Interdisciplinary Industrial Design Project II” at Kansas State University, supported by Westinghouse Electric Sweden. The authors would like to thank Dr. Mooneon Lee and Dr. Cheol Park of the KAERI for providing access to the report KAERI/TR-1665/2000.

## REFERENCES

1. N. E. TODREAS and M. S. KAZIMI, *Nuclear Systems Volume I: Thermal Hydraulic Fundamentals*, CRC Press, Boca Raton, FL, 3rd ed. (2021).
2. C. LEE and I. MUDAWAR, “A Mechanistic Critical Heat Flux Model for Subcooled Flow Boiling Based on Local Bulk Flow Conditions,” *International Journal of Multiphase Flow*, **14**, 6, 711–728 (1988).
3. Y. GUO and Y. ZHANG, “Review of Experimental and Numerical Studies on Critical Heat Flux in China,” *Energies*, **18**, 4, 781 (2025).

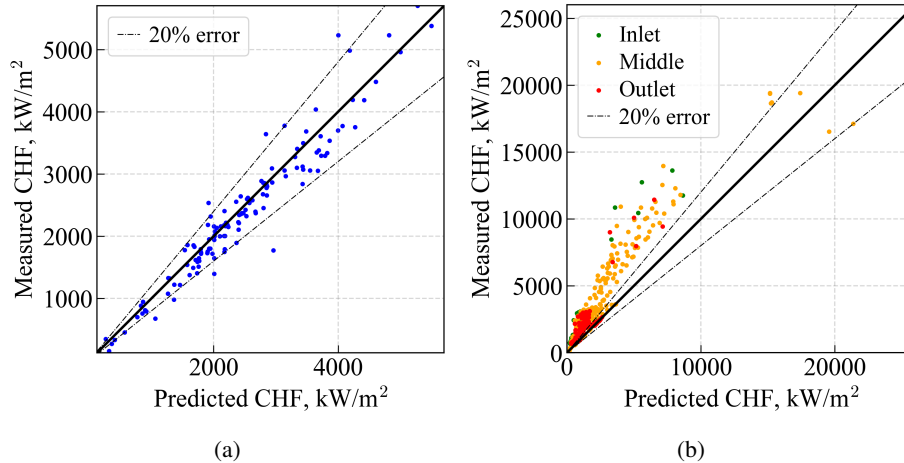


Fig. 3: Predicted vs. measured CHF using NN for (a) uniform data, (b) non-uniform data.

4. D. GROENEVELD, S. CHENG, and T. DOAN, “1986 AECL-UO Critical Heat Flux Lookup Table,” *Heat Transfer Engineering*, **7**, 1-2, 46–62 (1986).
5. D. GROENEVELD, J. SHAN, A. VASIĆ, L. LEUNG, A. DURMAYAZ, J. YANG, S. CHENG, and A. TANASE, “The 2006 CHF Look-Up Table,” *Nuclear Engineering and Design*, **237**, 15, 1909–1922 (2007), NURETH-11.
6. E. H. GROSFILLEY, G. ROBERTSON, J. SOIBAM, and J.-M. LE CORRE, “Investigation of Machine Learning Regression Techniques to Predict Critical Heat Flux Over a Large Parameter Space,” *Nuclear Technology*, pp. 1–15 (2024).
7. J.-M. LE CORRE, G. DELIPEI, X. WU, and X. ZHAO, “Benchmark on Artificial Intelligence and Machine Learning for Scientific Computing in Nuclear Engineering: Phase 1 Critical Heat Flux Exercise Specifications,” Tech. Rep. NEA/WKP(2023)1, OECD Nuclear Energy Agency (January 2024).
8. R. BOURISAW, R. MCCANTS, J.-M. LE CORRE, and A. S. ISKHAKOV, “Critical Heat Flux Prediction and Mitigation in Light Water Reactors,” Technical report, Kansas State University, Department of Mechanical and Nuclear Engineering (Jun. 2025), accessed: 2025-06-18.
9. C. PARK, “Effect of Axial Heat Flux Distribution on Critical Heat Flux,” Tech. Rep. KAERI/TR-1665/2000, Korea Atomic Energy Research Institute, Daejeon, Republic of Korea (October 2000).
10. H. S. SWENSON, J. R. CARVER, and C. R. KAKARALA, “The Influence of Axial Heat Flux Distribution on the Departure from Nucleate Boiling in a Water Cooled Tube,” in “ASME Winter Annual Meeting,” ASME (1963), 62-WA-297.
11. A. ROHATGI, “WebPlotDigitizer,” <https://automeris.io/WebPlotDigitizer> (2019), version 4.2; accessed June 16, 2025.
12. J. J. GÓMEZ-ROMERO, “IAPWS: Python Implementation of IAPWS-IF97 and Other Standards,” <https://pypi.org/project/iapws/> (2024), accessed: 2025-06-16.
13. R. BOURISAW, R. MCCANTS, J.-M. LE CORRE, A. ISKHAKOVA, and A. ISKHAKOV, “Critical Heat Flux Datasets under Uniform and Non-Uniform Axial Heating Conditions [KAERI/TR-1665/2000],” <https://doi.org/10.5281/zenodo.15691382> (2025).
14. R. W. BOWRING, “Simple but Accurate Round Tube, Uniform Heat Flux, Dryout Correlation over the Pressure Range 0.7 to 17 MN/m<sup>2</sup> (100 to 2500 psia),” Technical Report AEEWR789, Atomic Energy Establishment, Winfrith, England (1972), nTIS Issue Number 197223.
15. L. BIASI, G. C. CLERICI, S. GARRIBBA, R. SALA, and A. TOZZI, “Studies on Burnout. Part 3. A New Correlation for Round Ducts and Uniform Heating and Its Comparison with World Data,” *Energ. Nucl. (Milan)*, **14**, 530–536 (September 1967), oSTI ID: 4223933.